

Characterization and photoemission dichroism of epitaxially grown Gd(0001)/Y(0001)

S. R. Mishra^{a)}

Department of Physics, Virginia Commonwealth University, Richmond, Virginia 23284

T. R. Cummins and G. D. Waddill

Department of Physics, University of Missouri–Rolla, Rolla, Missouri 65401

K. W. Goodman and J. G. Tobin

Lawrence Livermore National Laboratory, Livermore, California 93550

W. J. Gammon, T. Sherwood, and D. P. Pappas

Department of Physics, Virginia Commonwealth University, Richmond, Virginia 23284

(Received 13 October 1997; accepted 8 December 1997)

Gadolinium thin films approximately 100 Å thick have been grown epitaxially on a Y(0001) substrate. A threefold characterization has been performed. The surface structural analyses of the yttrium substrate and the gadolinium films were performed using x-ray photoelectron diffraction (XPD) and low-energy electron diffraction (LEED). The results of the XPD and LEED studies strongly suggest that gadolinium films have an effective C_{6v} surface symmetry, consistent with earlier studies of other hcp (0001) surfaces. The elemental analysis of the substrate and the film was done with x-ray photoemission using Mg, Al $K\alpha$ x rays and synchrotron radiation. The magnetic analysis is based upon magnetic x-ray dichroisms observed in angle-resolved photoelectron spectroscopy, using both linearly polarized and circularly polarized synchrotron x-ray radiation as the excitation. Photoemission from the Gd 4*f* and 5*p* core-level states were used in this magnetic characterization and will be presented. This includes novel magnetic linear dichroism angular distribution results for the Gd 5*p*, which exhibit up to 40% asymmetry, on a par with the previously reported circular dichroism results. © 1998 American Vacuum Society. [S0734-2101(98)01603-0]

I. INTRODUCTION

Surface magnetism is an interesting phenomenon resulting from the rearrangement of the surface atoms, thus producing different magnetic ordering than in the bulk. In particular, the surfaces of rare-earth metals have been heavily investigated because of their novel magnetic properties such as enhanced magnetization at the surface, imperfect ferromagnetic alignment of the surface with the bulk,^{1,2} and different magnetic coupling at the surface, as opposed to that within the bulk. However, the studies of surface phenomenon of rare-earth films present a challenge to the experimentalist owing to the strong chemical reactivity of the rare-earth elements, which makes it difficult to grow a clean and well-ordered thin film, avoiding interdiffusion with the substrate and maintaining an atomically clean surface and film.³

Here, we report the results of an investigation of the structure, elemental composition, and magnetic properties of gadolinium thin films grown on a yttrium (0001) substrate. The attraction to study gadolinium comes from the possibility of a simple atomiclike configuration, which has seven unpaired electrons in the ground-state $4d^{10}5s^25p^64f^7$ configuration. In this case, the spin of all seven 4*f* electrons are aligned, giving a total spin angular momentum number of 7/2 and total orbital momentum number of zero. As a result of this high spin state, Gd has the largest magnetic moment of the rare earths, close to 8 μ_B .⁴ As the 4*f* shell electrons are

screened by the valence 5*d* and 6*s* electrons, gadolinium is an excellent example of a local ferromagnet, having a bulk Curie temperature of $T_c = 293$ K.

The surface magnetic properties of Gd are strongly dependent on the geometric arrangement of the surface atoms. It was observed by Weller *et al.*⁵ that Gd(0001) films grown on W(110) show a magnetic surface reconstruction leading to an enhanced surface Curie temperature of 315 K, or 22° higher than the bulk. The higher surface Curie temperature was attributed to the enhanced magnetic order at the surface.⁶ However, the growth condition, postannealing, and the quality of the Gd film do play an important role in enhancing the surface magnetic order. Scanning tunneling microscopy investigations carried out by Tober and co-workers^{7,8} have shown that gadolinium grows in a multilayer mode rather than layer by layer on W(110). Also, the postannealing of the resulting films produces monatomically stepped surfaces or three-dimensional islands depending upon the annealing temperature. They further show that relative to bulk Gd, the Gd monolayer is expanded by 1.2% along the W[001] direction and compressed by 0.6% along the $[-110]$ direction, thus leading to corrugated film growth. In order to eliminate the substrate strain effect on the growth of the gadolinium film and its subsequent complications, we have chosen a close lattice-matched yttrium substrate, which should lead to an epitaxial, layer-by-layer, Frank–Van der Merve growth and thus strain-free growth of the film.

^{a)}Electronic mail: sanjay@b17-36.als.lbl.gov

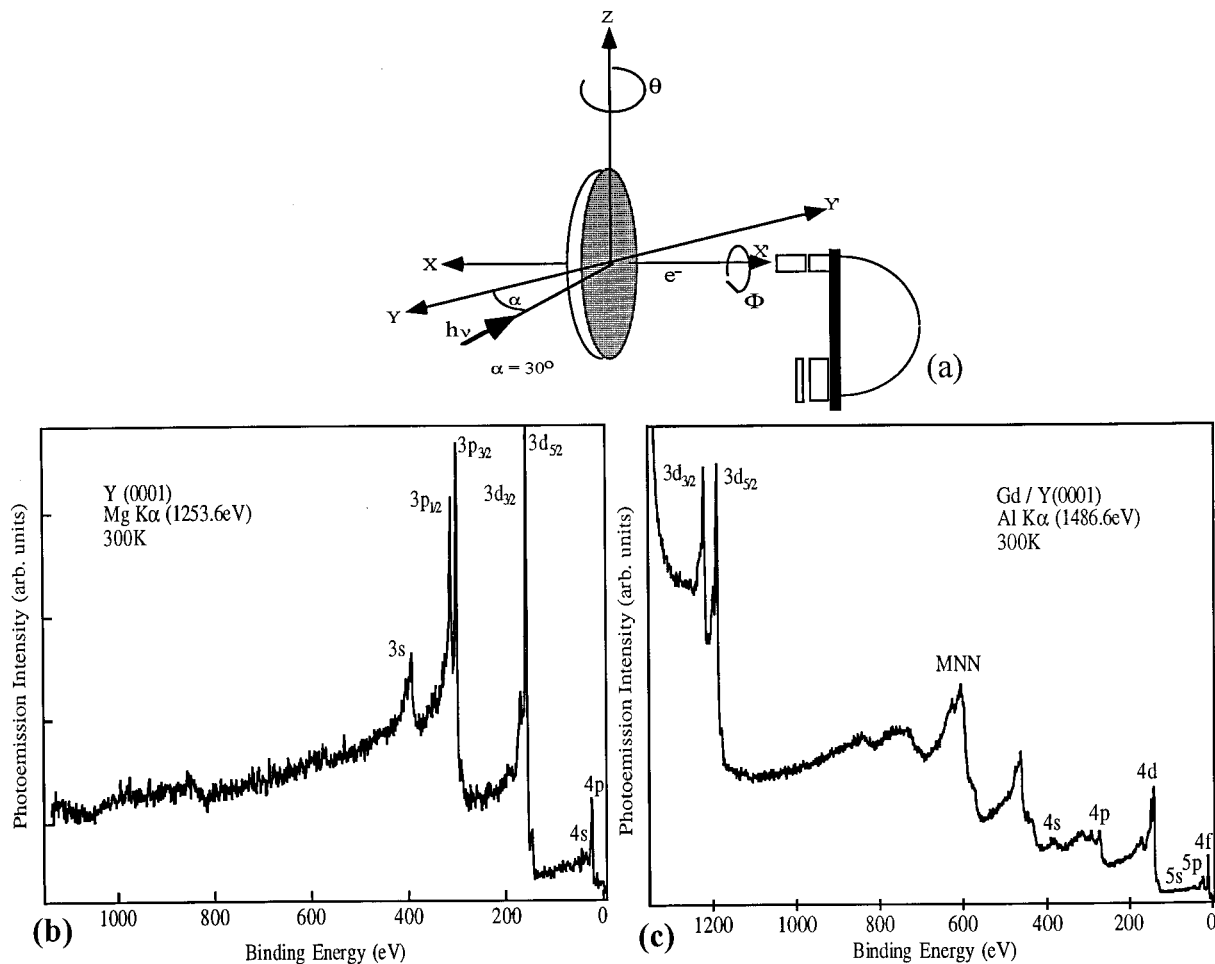


FIG. 1. (a) Experimental geometry for synchrotron radiation photoelectron spectroscopy and Al/Mg $K\alpha$ XPS: The synchrotron x rays are incident at an angle 30° relative to the YY' axis. The photoelectrons are collected along the sample normal to the direction. The angle of incidence for the Al and Mg $K\alpha$ radiation is 45° above the horizontal plane and at an angle 55° in the horizontal plane. The Al and Mg $K\alpha$ scans were also collected at normal emission. (b) Mg $K\alpha$ (1253.6 eV) XPS spectrum from a Y(0001) substrate for sample B. In this case, small oxygen, fluorine, and chlorine contaminants are present. (c) Al $K\alpha$ (1486.6 eV) XPS spectrum from Gd(0001)/Y(0001), sample B. Note the lack of contamination.

The magnetic properties of Gd(0001)/Y(0001) were probed using magnetic dichroism in an angular distributions technique,^{9–27} a photoelectron spectroscopy based technique which obviates the need of spin detection by exploiting the difference of angular distribution of photoelectrons induced by magnetization reversal. Thus, this spectroscopy measures an intensity difference reflecting changes in spin polarization. The linear dichroism experiment is performed in a chiral geometry where the magnetization vector is orthogonal to the plane containing the Poynting vector and the linear polarization of the incident photon as well as the emission direction of the electrons. In the circular dichroism experiment [magnetic circular dichroism angular distribution (MCDAD)] the Poynting vector and the helicity of the photons and the sample magnetization are approximately collinear.^{14–20} We report MCDAD results for the Gd 5*p* level, including in the photon energy range corresponding to the Gd 4*d*–4*f* transitions, which can give rise to resonant photoemission. Our results will be compared to those previously reported magnetic linear dichroism angular distribution

(MLDAD)^{21,22} and MCDAD^{23,24} in the 4*f* and MCDAD^{25,26} in 5*p* core-level photoemission.

II. EXPERIMENT

The photoelectron experiments were conducted at the Spectromicroscopy Facility, Beamline-7, of the Advance Light Source Facility in Berkeley, CA at Lawrence Berkeley National Laboratory.^{27,28} Beamline-7 is located at an undulator port, providing the source of tunable linearly polarized soft x rays. Circularly polarized x radiation at 95 eV is generated using a novel phase retarder.²⁹ A diagram of the experimental geometry is shown in Fig. 1(a). The x rays are incident at an angle of 30° from the *Y* axis. In the linear polarization experiments the electric-field vector **E** is in the *xy* plane. In the circular dichroism experiment the helicity is parallel or antiparallel to the Poynting vector of the photon. Photoelectrons are collected at normal emission along the *x* axis with 2° resolution, with the intensity normalized to the photon flux by an Au mesh drain current measured upstream.

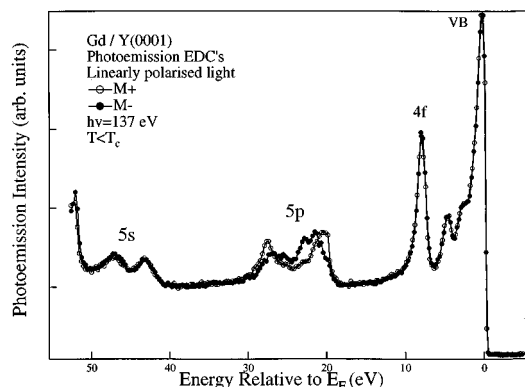


FIG. 2. Normal emission synchrotron radiation photoemission from Gd(0001)/Y(0001) at a photon energy of 137 eV. Two configurations are shown, with the magnetization along $+Z$ and $-Z$. The sample was rotated 180° to achieve magnetization reversal. Besides the Gd derived peaks, oxygen-related features at a binding energy of about 5 eV are apparent, plus the front edge of the Fe $3p$ core level at a binding energy of 53 eV.

In all dichroism experiments, the magnetization \mathbf{M} lies in the plane of the sample: in the MLDAD experiments, \mathbf{M} is along $+/-Z$, positioned orthogonal to the electric-field vector of the exciting radiation; in the circular dichroism experiments, \mathbf{M} is along $+/-Y$. We have assumed that the magnetization is, in fact, in the plane of the surface along $[11-20]$ a direction corresponding to $[11-20]$ of the Y(0001) surface. This assumption remains under investigation.

The yttrium crystal was aligned by Laue diffraction and mechanically polished with a $1\ \mu\text{m}$ diamond solution. The crystal was mounted on a two-axes manipulator allowing variations of polar (Θ) and azimuthal (Φ) rotation necessary to perform x-ray photoelectron diffraction (XPD) and the change of magnetization direction required for the dichroism experiments. The yttrium substrate was cleaned *in situ* by sputtering with a 1.5 keV beam of argon ions and then annealed at 875 K.

Gadolinium thin films $\sim 100\ \text{\AA}$ were grown at room temperature on a Y(0001) crystal using an e-beam evaporator. An approximately $100\ \text{\AA}$ film was grown because the Curie point is expected to be significantly reduced from the bulk value of 293 K for thin Gd films $< 15\ \text{ML}$.³⁰ The film thickness was monitored by quartz-crystal microbalance. The film was grown at the rate of $15\ \text{\AA}$ per minute. The base pressure rose from 5×10^{-10} to 3×10^{-9} Torr during deposition. The film was ordered by a short anneal of 45 s at 710 K. The quality of the substrate as well as of the film was checked via x-ray photoelectrons excited using Mg $K\alpha$ and Al $K\alpha$ radiation, respectively. The crystallinity of the film was monitored via low-energy electron diffraction (LEED) and XPD. The Gd films were magnetized in plane by the pulses of 100 kOes from a nearby solenoid. All magnetic measurements were made in remanence. From previous studies of Gd(0001)/W(0001), the magnetization of the film is expected to lie in the plane in a single-domain state.³¹ Two samples were prepared: A and B. They will be described in the section to follow. The samples were cooled with liquid nitrogen, with an estimated temperature around 250 K.

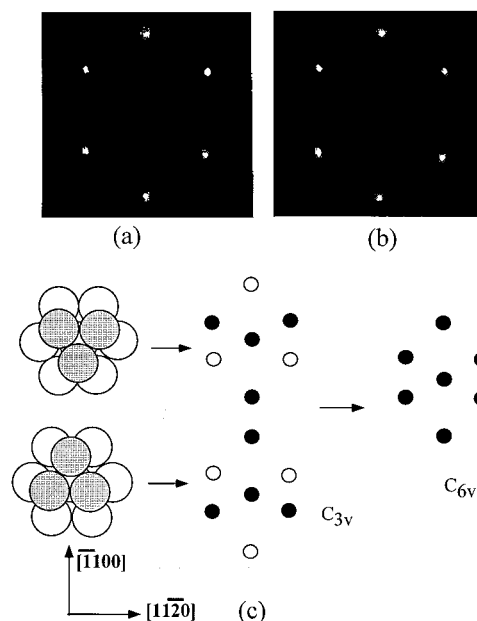


FIG. 3. (a) LEED pattern from Y(0001) at 44 eV primary beam energy, (b) LEED pattern from Gd(0001)/Y(0001) at 49 eV primary beam energy. (c) Schematic representation of the relation between the structure and the LEED pattern observed for the hcp (0001) surface. The superposition of LEED patterns generated by two possible terminations of the surface atoms leads to the sixfold symmetric LEED pattern. The experimental LEED patterns are taken from the Masters thesis of Sherwood.

III. RESULTS AND DISCUSSION

A. Elemental analysis

The preparation of clean and well-ordered single-crystalline rare-earth metal is a delicate matter due to the high chemical reactivity of rare-earth metals. Spin-resolved photoemission experiments by McIlroy *et al.*³² have shown that a Gd(0001) surface exposed to as little as 0.25 ML of oxygen forms an oxide with reduced magnetic properties, thus, elimination of surface contaminants is essential. There are basically two sources of contamination: one from the surrounding ultrahigh vacuum environment such as carbon, oxygen, and hydrocarbons and the other from the bulk such as chlorine, fluorine, and iron. The contaminant from the surrounding can be well avoided by carrying out the experiment in a "clean" experimental chamber where exposed parts are properly baked and outgassed. The inherent impurities are difficult to remove as they readily diffuse out to the surface upon annealing.

In order for gadolinium to grow epitaxially on the substrate it is necessary to have a contaminant-free substrate. Repeated sputter anneal cycles for long hours can drain out bulk impurities. However, it is unlikely to get rid of all these impurities. X-ray photoemission spectroscopy (XPS) performed on a preannealed yttrium substrate, which was carried through 20 h of sputter/anneal cycles show the presence of a substantial amount of oxygen and a small amount of iron. Annealing the substrate at 875 K eliminated oxygen from the surface, but this high annealing temperature allowed iron to diffuse on the crystal surface. A Mg $K\alpha$ XPS

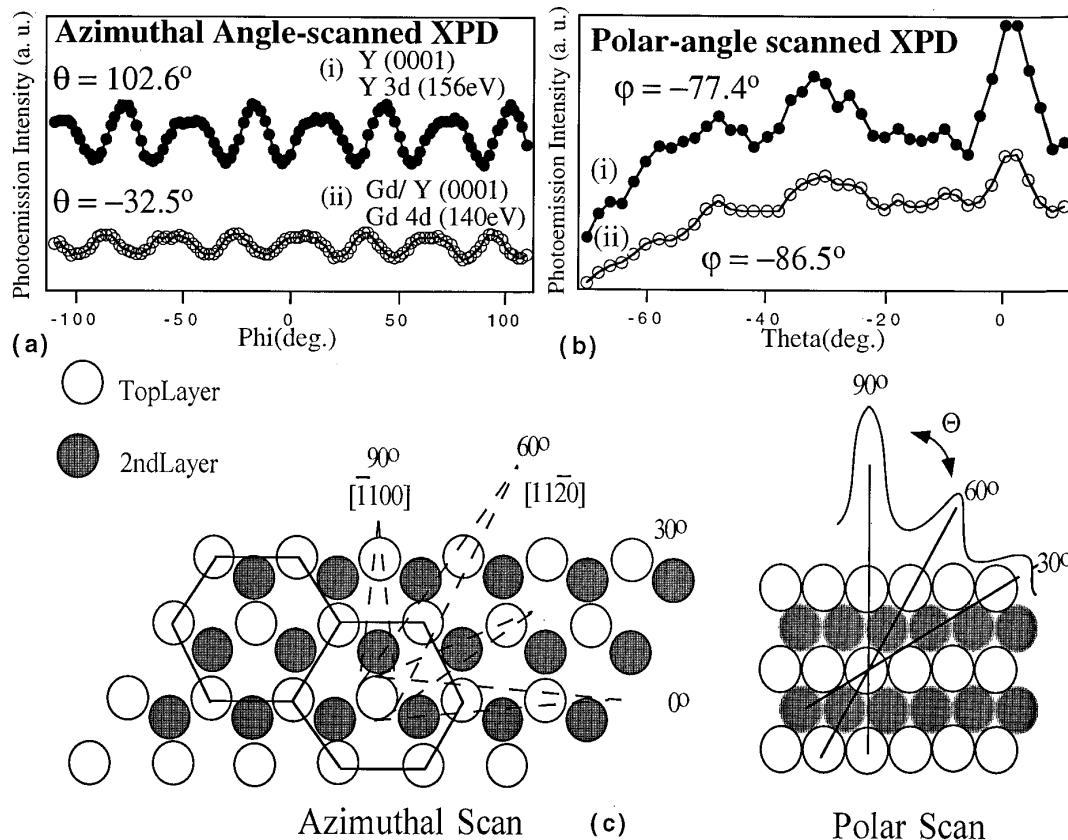


FIG. 4. XPD of the clean Y(0001) surface and Gd(0001)/Y(0001) film. (a) Azimuthal-angle scans. (b) Polar-angle scans. Both sets of data were collected using the sample A substrate and Mg $K\alpha$ radiation (1253.6 eV). (c) The schematic representation of forward scattering events in hcp stacking for azimuthal and polar-angle scans.

of a thin Gd film grown on this substrate (sample A) also shows the presence of iron contamination, which possibly diffused out from the yttrium substrate upon annealing. With much longer hours of the sputter/anneal cycle we were able to produce a yttrium substrate that was fairly free of oxygen and iron contamination, Fig. 1(b). During this cycle, the substrate was annealed at lower temperature but high enough to reorder the surface. However, we were unable to completely eliminate halide contamination from the surface. An Al $K\alpha$ XPS of a thin gadolinium film grown on this substrate (sample B) does not show any trace of oxygen, iron, or halide contamination, Fig. 1(c). It is possible that iron may remain undetected due to a low photoionization cross section of core levels at Al $K\alpha$ radiation.³³ The XPS spectra obtained at 137 eV using synchrotron x rays show less than a few percent of iron contamination on the Gd(0001)/Y(0001) film, Fig. 2. Thus, it is advisable to check for contaminants at the photon energy where its core-level photoionization cross section is maximum. Also, the annealing temperature could be optimized to produce a well-ordered surface without segregating iron on the yttrium surface. While sample B exhibited a fairly high degree of cleanliness, the sample A surface exhibited worse contamination, particularly from iron.

B. Geometric structure

The surface ordering of the substrate plays an important role in the growth of an epitaxial film. Thus, it is important

to perform an analysis of the substrate surface before growing an epitaxial film on it. LEED and XPD³⁴ are suitable techniques to study the surface structure as the former is surface sensitive because of the large elastic cross section of electrons (approximately 1 Å), the latter is fairly surface sensitive but elementally specific. LEED patterns from a clean Y(0001) surface and Gd(0001)/Y(0001) at 44 and 49 eV, respectively are shown in Fig. 3. The sharp (1×1) patterns implies the existence of a well-ordered Y(0001) surface and Gd(0001)/Y(0001) film and provides information about the symmetry of the surface. In both cases, the LEED pattern indicates that the surface has a sixfold symmetry but the true surface structure possesses a lower local symmetry as suggested by Shih *et al.*³⁵ for hexagonal close-packed-type atomic stacking. This situation occurs when the surface contains two domains and are oriented with respect to one another precisely by a symmetry operation. As shown in Fig. 3(c), the “ideal” hcp(0001) stacking exhibits two different LEED patterns depending on the way in which the bulk is terminated. The two patterns have threefold C_{3v} -type symmetry rotated by 60° with respect to one another. The composite effect appears as an effective sixfold symmetry of a C_{6v} -type arrangement of atoms on the surface.

The result of XPD studies of the Y(0001) and the Gd(0001)/Y(0001) is shown in Fig. 4. The XPD measurements were performed in an angle scanned mode using the yttrium 3d and gadolinium 4d photoemission lines for sub-

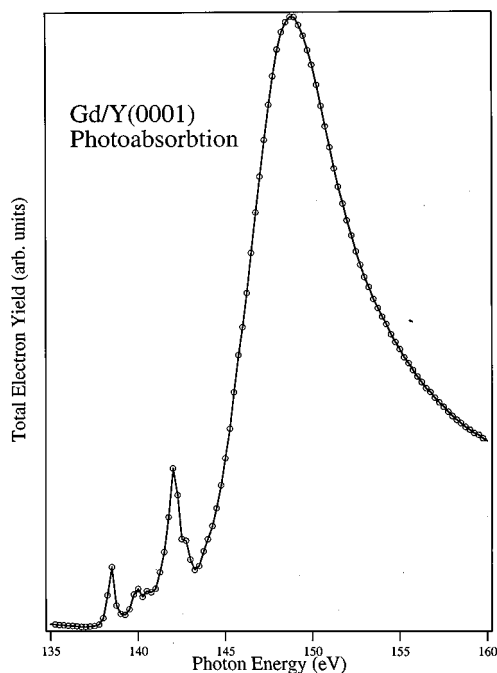


FIG. 5. An x-ray absorption spectrum of Gd(0001)/Y(0001) recorded in a total electron yield mode. The prepeak structure occurs around photon energies of 135–143 eV and the giant resonance is at a photon energy of 148 eV. The spectrum was taken from the Masters thesis of Gammon.

strate and film, respectively, with excitation via Mg $K\alpha$ radiation. The XPD technique is based on the principle of forward focusing where the outgoing core-level or Auger photoelectron intensities are enhanced along the azimuthal and polar angles corresponding to the direction connecting the emitting atom with its nearest and next-nearest atoms.^{18,36} Since the core-level peaks are element specific, observation of the direction in which their intensities are enhanced constitute a local probe of the structural environment around the emitting atom. The forward scattering events for the hcp structure of Y(0001) and Gd(0001)/Y(0001) observed in azimuthal and polar scans is illustrated in Fig. 4(c), together with a schematic diagram, which qualitatively explains the observed XPD patterns. Notice that in the azimuthal-angle scan, the forward focusing event produces intense peaks at 60° and 0° and less intense peaks at 90° and 30° corresponding to the direction $[11\bar{2}0]$ and $[\bar{1}100]$, respectively. The less intense peaks at 90° and 30° result from the scattering events from atoms farther away from the emitter. The repetition of peaks at every 60° indicate that on the average the emitter atom is located in a sixfold symmetric environment of the neighboring atoms. Similarly, a qualitative explanation for the polar-angle scan pattern observed for the Y(0001) and Gd(0001)/Y(0001) is illustrated in Fig. 4(c). For the observed sixfold symmetric XPD pattern of the Y(0001) substrate and the Gd(0001)/Y(0001) film we suggest that gadolinium film deposits epitaxially layer-by-layer on the Y(0001) substrate and not by island formation. The true epitaxial growth of the film is hard to achieve due to the presence of surface defects and steps.

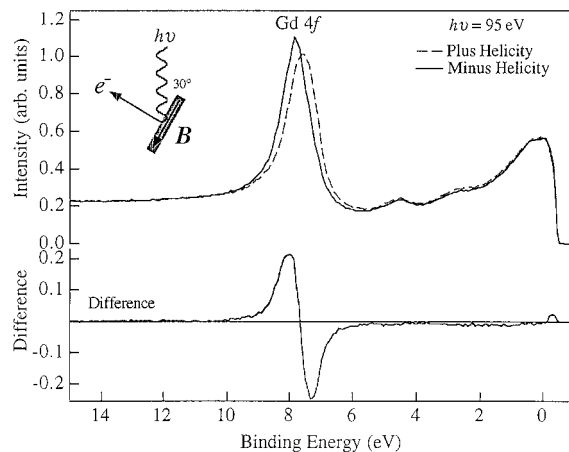


FIG. 6. The MCDAD in the photoemission electron distribution curves of Gd(0001)/Y(0001) at a photon energy of 95 eV for parallel and antiparallel arrangement of photon helicity and magnetization. The raw spectra and difference curves are shown. A peak-to-peak asymmetry of 20% is shown.

During the film growth, these surface defects and steps introduce stress in the film. The observed reduction in the XPD intensity of the Gd(0001)/Y(0001) film may be linked to disorder in the film.

Using the XPD scans, a “mirror” plane was chosen for the MLDAD and MCDAD experiments. The magnetization vector was then induced in the plane of the surface, perpendicular to the mirror plane. The presence of the effective C_{6v} mirror plane is essential to both the MCDAD and MLDAD experiments. As we performed them, in the MCDAD experiment, we reversed helicity instead of flipping the magnetiza-

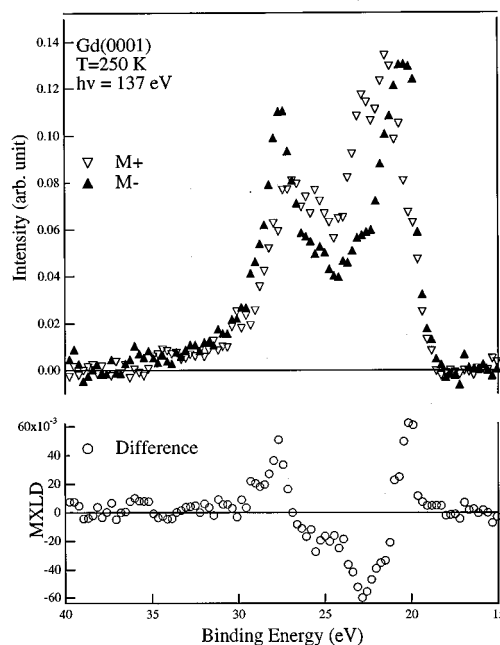


FIG. 7. The MLDAD in the photoemission of Gd 5p from Gd(0001)/Y(0001) in the prepeak region is shown here. The photon energy was 138 eV. This is an expansion of the 5p peak shown in Fig. 2. Here, asymmetry of 30% was observed.

tion. In the MLDAD experiment, magnetization reversal was achieved by rotating the sample azimuthally 180° instead of reversing the magnetization via an opposite magnetic-field pulse.

C. Dichroism in angle-resolved photoemission spectroscopy

A series of magnetic dichroism experiments have been performed in the vicinity of the Gd $4d-4f$ resonance as indicated in the yield curve in Fig. 5. MCDAD was performed using 95 eV photons for both parallel and antiparallel alignment of photon helicity and magnetization as shown in Fig. 6. Strong effects are observed in Gd $4f$ photoemission with experimental asymmetries up to 12%, comparable to that observed previously by Starke *et al.*¹⁶ The effects seen have been thoroughly described previously.²⁶ As shown in Ref. 22, MLDAD in $4f$ photoemission have been recorded for photon energies in the vicinity of the giant resonance. The observed multiplets in the preedge region of the giant resonance have been successfully explained within atomic multiplet calculations.³⁷ The MLDAD asymmetries are observed up to 10% both on- and off-resonance (not shown), with significant changes in intensity and line-shape details as one traverses the respective energy range.^{22,38} In Fig. 7, we present preliminary MLDAD in Gd $5p$ photoemission corresponding to photon energies in the preedge region of the $4d-4f$ giant resonance.^{39,40} Asymmetries of up to 30%, comparable to the results of Arenholz and co-workers has been observed.^{25,26} We have also recorded MLDAD in $5p$ photoemission as a function of photon energies in the region of the $4d-4f$ giant resonance. We are currently performing analysis on these results which, will form the subject of our forthcoming article.⁴¹

ACKNOWLEDGMENTS

This work was performed under the auspices of the U.S. Department of Energy by Lawrence Livermore National Laboratory under Contract No. W-7405-Eng-48. Experiments were carried out at the Spectromicroscopy Facility (Beamline 7.0) at the Advance Light Source, built and supported by the U.S. Department of Energy.

¹G. A. Mulhollan, K. Garrison, and J. L. Erskine, Phys. Rev. Lett. **69**, 3240 (1992).

²H. Tang, D. Weller, T. G. Walker, J. C. Scott, C. Chappert, H. Hopster, A. W. Pang, D. S. Dessau, and D. P. Pappas, Phys. Rev. Lett. **71**, 446 (1993).

³B. J. Beaudry and K. A. Gschneidner, in *Handbook of Physics and Chemistry of Rare Earths*, edited by K. A. Gschneidner and L. R. Eyring (North-Holland, Amsterdam, 1978), Vol. 1.

⁴See for example, N. W. Ashcroft and N. D. Mermin, in *Solid State Physics*, (Holt-Saunders, New York, 1981), p. 657.

⁵D. Weller, S. F. Alvarado, W. Gudat, K. Schröder, and M. Campagna, Phys. Rev. Lett. **54**, 1555 (1985).

⁶P. A. Dowben, D. N. McIlroy, and Dongqi Li, in *Handbook of the Physics and Chemistry of Rare Earths*, edited by K. A. Gschneidner and L. R. Eyring (North Holland, Amsterdam, 1995), Vol. 24.

⁷E. D. Tober, R. X. Ynzunza, C. Westphal, and C. S. Fadley, Phys. Rev. B **53**, 5444 (1996).

⁸E. D. Tober, R. X. Ynzunza, F. J. Palomares, Z. Wang, Z. Hussain, M. A. Van Hove, and C. S. Fadley, Phys. Rev. Lett. **79**, 2085 (1997).

⁹Ch. Roth, F. U. Hillebrecht, H. B. Rose, and E. Kisker, Phys. Rev. Lett. **70**, 3479 (1993); Solid State Commun. **86**, 647 (1993); F. U. Hillebrecht, H. B. Rose, T. Kinoshita, Y. U. Idzerda, G. van der laan, R. Denecke, and L. Ley, Phys. Rev. Lett. **75**, 2883 (1995); F. U. Hillebrecht, C. Roth, H. B. Rose, W. G. Park, E. Kisker, and N. A. Cherepkov, Phys. Rev. B **53**, 12182 (1996).

¹⁰B. T. Thole and G. van der Laan, Phys. Rev. Lett. **67**, 3306 (1991); G. van der Laan, Phys. Rev. B **51**, 240 (1995).

¹¹W. Kuch, M. T. Lin, W. Steinhogel, C. M. Schneider, D. Venus, and J. Kirschner, Phys. Rev. B **51**, 609 (1995).

¹²G. Rossi, F. Sirotti, N. A. Cherepkov, F. Cambet-Famoux, and G. Panacione, Solid State Commun. **90**, 557 (1994); F. Sirotti and G. Rossi, Phys. Rev. B **49**, 15 682 (1994).

¹³J. G. Tobin, K. W. Goodman, G. J. Mankey, R. F. Willis, J. D. Denlinger, E. Rotenberg, and A. Warwick, J. Appl. Phys. **79**, 5626 (1996); J. Vac. Sci. Technol. B **14**, 3171 (1996).

¹⁴L. Baumgarten, C. M. Schneidner, M. Petersen, F. Schafers, and J. Kirschner, Phys. Rev. Lett. **65**, 492 (1990).

¹⁵G. D. Waddill, J. G. Tobin, and D. P. Pappas, Phys. Rev. B **46**, 552 (1992).

¹⁶K. Starke, L. Baumgarten, E. Arenholz, E. Navas, and G. Kaindl, Phys. Rev. B **50**, 1317 (1994); K. Starke, E. Navas, L. Baumgarten, and G. Kaindl, Phys. Rev. B **48**, 1329 (1993).

¹⁷C. M. Schneider, D. Venus, and J. Kirschner, Phys. Rev. B **45**, 5041 (1992).

¹⁸G. D. Waddill, J. G. Tobin, X. Guo, and S. Y. Tong, Phys. Rev. B **50**, 6774 (1994).

¹⁹J. G. Tobin, G. D. Waddill, E. Tamura, P. Sterne, P. J. Bedrossian, D. P. Pappas, X. Guo, and S. Y. Tong, Surf. Rev. Lett. **3**, 1429 (1996).

²⁰X. Le Cann, C. Boeglin, B. Carriere, and K. Hricovini, Phys. Rev. B **54**, 373 (1996).

²¹T. Kinoshita, H. B. Rose, C. Roth, F. Ulrich, and E. Kisker, J. Electron Spectrosc. Relat. Phenom. **8**, 333 (1996).

²²W. J. Gammon, S. R. Mishra, D. P. Pappas, K. W. Goodman, J. G. Tobin, F. O. Schumann, R. Willis, J. D. Denlinger, E. Rotenberg, A. Warwick, and N. Smith, J. Vac. Sci. Technol. A **15**, 1 (1997).

²³E. Arenholz, E. Navas, K. Starke, L. Baumgarten, and G. Kaindl, Phys. Rev. B **51**, 8211 (1995).

²⁴K. Starke, E. Navas, E. Arenholz, Z. Hu, L. Baumgarten, G. van der Laan, C. T. Chen, and G. Kaindl, Phys. Rev. B **55**, 2672 (1997).

²⁵E. Arenholz, in *Magnetic Dichroism in Photoemission from Lanthanide Materials: Basic Concepts and Applications* (Wissenschaft und Technik, Berlin, 1996).

²⁶G. van der Laan, E. Arenholz, E. Navas, Z. Hu, E. Mentz, A. Bauer, and G. Kaindl, Phys. Rev. B **56**, 3244 (1997).

²⁷J. G. Tobin, K. W. Goodman, G. J. Mankey, R. F. Willis, J. D. Denlinger, E. Rotenberg, and A. Warwick, J. Appl. Phys. **79**, 5626 (1996).

²⁸J. D. Denlinger, E. Rotenberg, T. Warwick, G. Visser, J. Nordgren, J. H. Guo, P. Skytt, S. D. Kevan, K. S. McCutcheon, D. Shuh, J. Bucher, N. Edelstein, J. G. Tobin, and B. P. Toner, Rev. Sci. Instrum. **66**, 1342 (1995).

²⁹J. G. Kortright, H. Kimura, V. Nikitin, K. Mayama, M. Yamamoto, and M. Yanagihara, Appl. Phys. Lett. **60**, 2963 (1992); J. B. Kortright and J. H. Underwood, Nucl. Instrum. Methods Phys. Res. A **291**, 272 (1990).

³⁰M. Farle, K. Babershe, U. Stetter, A. Aspelmeier, and F. Gerhardt, Phys. Rev. B **47**, 11 571 (1993).

³¹A. Berger, A. W. Pang, and H. Hopster, Phys. Rev. B **52**, 1078 (1995).

³²D. N. McIlroy, C. Walfried, Donqui Li, J. Pearson, S. D. Bader, D. J. Hung, P. Jhonson, R. F. Sabiryanov, S. S. Jaswal, and P. A. Dowben, Phys. Rev. Lett. **76**, 2802 (1996).

³³J. J. Yeh and I. Lindau, At. Data Nucl. Data Tables **32**, 1 (1985).

³⁴C. S. Fadley, in *Synchrotron Radiation Research: Advances in Surface Science*, edited by R. Z. Bachrach (Plenum, New York, 1990).

³⁵H. D. Shih, F. Jona, D. W. Jepsen, and P. M. Marcus, J. Phys. C **9**, 1405 (1976).

³⁶For example, W. F. Egelhoff, Jr., Crit. Rev. Solid State Mater. Sci. **16**, 213 (1990).

- ³⁷F. Gerken, J. Barth, and C. Kunz, Phys. Rev. Lett. **47**, 993 (1987).
- ³⁸W. J. Gammon, Thesis, Virginia Commonwealth University, Richmond, 1996.
- ³⁹B. T. Thole, X. D. Wang, B. N. Harmon, Dongqi Li, and P. A. Dowben, Phys. Rev. B **47**, 9098 (1993).
- ⁴⁰Dongqi Li and P. A. Dowben, Mater. Res. Soc. Symp. Proc. **231**, 107 (1992), P. A. Dowben, D. LaGrafte, and M. Onellion, J. Phys.: Condens. Matter **1**, 6571 (1989).
- ⁴¹T. R. Cummins, S. R. Mishra, G. D. Waddill, K. W. Goodman, J. G. Tobin, W. J. Gammon, T. Sherwood, and D. P. Pappas (unpublished).